Design and MHD Modeling of ATLAS experiments to Study Friction

R. J. Faehl[1] and J. E. Hammerberg[2]
Plasma Physics Group[1] and Materials Science Group[2], Los Alamos National Laboratory,
Los Alamos New Mexico 87545

Abstract

Transverse shear at the interface of two solids occurs when these solids move at different velocities. This frictional phenomenon is being studied in a series of experiments on the ATLAS capacitor bank at Los Alamos. Cylindrical targets to test friction force models are composed of alternating regions of high- and low-shock speed materials. When the target is impacted by a cylindrical, magnetically-accelerated aluminum liner, the differential shock velocity in the two materials establishes the desired shear at the interface. One- and two-dimensional MHD calculations have been performed to design liners with suitable properties to drive these "friction-like" ATLAS experiments. A thick impactor allows the shock to be maintained for several microseconds. The ATLAS experiments use a liner that is approximately 10 mm thick at impact, with an inner surface velocity of ~1.4-1.5 km/s. Interaction of this thick liner with the electrodes, or glide planes, results in significant deformation of the hardened stainless steel electrodes. Data from the ATLAS experiments and comparisons with the calculations will be presented, along with plans for future experiments.

I. Introduction

When two solid surfaces slide against each other transverse shear stresses are generated at the interface. These stresses are then transmitted into the material interiors. For ductile materials, this process is due to production of dislocations, within the material lattice. Macroscopically, it leads to the phenomenon commonly known as friction.

In this paper, we briefly describe the phenomenon believed to be responsible for friction, in different velocity regimes. From such regimes, Hammerberg, et. al.[1] have constructed a model for dynamic friction. We then describe the process of designing experiments for the ATLAS pulsed-power system[2] that should be able to provide data against which the model can be tested. Finally we describe some of the calculations performed to predict the dynamic behavior of the liner (ie. driver) and its interaction with the friction target.

II. Description of the Friction Model.

The low velocity regime for interface sliding, at least for relatively flat interfaces, may be analyzed in terms of linear response theory, of the phonon distribution to external perturbation. This gives rise to a generally increasing dependence of the frictional force with velocity[3]. At high velocities (ie. greater than about 10% of the sound speed), more dramatic dynamic effects become important, involving dislocation patterning and graded microstructural evolution under dynamic loading. Simple arguments based upon the high rate behavior of the flow stress and stress localization characterized by a dense distribution of dislocations lead to a prediction of a power law decrease of the frictional force with velocity, so that the tangential force $Ft \sim v^{-(1-\alpha)}$ where α is the exponent of the very high plastic strain rate dependence of the flow stress, τ, $\tau \propto \varepsilon_p^{\alpha}$ [4]. For many metals, $\alpha \approx 1/4$ [5]. In an intermediate velocity regime, one expects a crossover in behavior with velocity giving rise to a maximum in Ft. This picture is in agreement with the large scale molecular dynamics (MD) simulations that have been performed on relatively flat interfaces.

However experiments in this regime of high velocities are very difficult. We describe the process that went into designing our experiments, to provide data to test the above model.

III. Experimental Design Criteria.

This new friction model has motivated us to design a series of experiments to test its quantitative aspects. These experiments are all in cylindrical geometry with azimuthal symmetry. The sliding interfaces are at the axial boundaries of "lifesaver"-shaped cylinders, composed of different materials. Different material speeds are induced in individual cylinders by shocking the outer radial surfaces simultaneously. This target assembly is therefore composed of alternating cylindrical blocks of different materials. The target assembly is shown schematically in Figure 1.

In general, we choose one of the materials with a relatively high sound speed, and the other with a much lower sound speed. Aluminum is a good choice for the high sound speed material, with a bulk sound speed of 5.24 km/s (the Al-6016 T6 alloy). There are a few materials with higher sound speeds, but they tend to have other undesirable properties from either fabrication or health/safety features. Beryllium, for instance, has a bulk sound speed of 8.0 km/s but is a highly toxic material. There are a number of resasonable candidate materials for the low sound speed side of the target. Gold and silver both have sounds speeds on the order of 3 km/s. Tantalum was chosen for the first experiments because it has a low sound speed (3.41 km/s), is not difficult to machine, and is not excessively expensive. The absolute magnitudes of sound speed are not the important metric; the primary factor is the difference in sound speeds between adjacent materials. Certain combinations of materials, such as aluminum and titanium (5.02 km/s), are automatically excluded from study with this technique.

The shock that induces the differential speeds at the interfaces is generated by a cylindrically imploding impactor which hits the outer target surface. We can relate the shock speed, U, to the velocity of the impactor, v_I,

$$U = S_1 v_I + S_2 v_I^2 + \ldots \qquad (1),$$

where for a Gruneisen Equation of State (EOS), the strength formulation due to Steinburg [6] gives $S_1 = 1.4$ for aluminum and $S_1 = 1.2$ for tantalum ($S_j \cong 0$, for $j \geq 2$). There is no particular reason to believe that the Gruneisen EOS is most appropriate for describing these materials but it allows a convenient analytic measure.

The target materials determine the relative magnitude of velicity difference across the interface. The model described in Section II must be used to determine which impactor velocity is useful. For aluminum and tantalum, $v_I \cong 1.4$-1.5 km/s provides a critical test for the model.

The experiments that we discuss in this paper are cylindrical targets. This is not the only possible geometry. Planar target experiments can also be conducted. Such a target would be shocked by a flyer plate, which is accelerated by a gas gun. The "flyer plate" in this set of experiments is a cylindrical aluminum liner, accelerated by magnetic pressure from a pulsed power source. Previous experiments[2] in converging geometry assemblies were conducted using the, now-decommissioned PEGASUS II capacitor bank. While these experiments were quite promising, the PEGASUS machine proved to be energy-limited. This limitation resulted in a less-than optimum experimental configuration: the liner was only 4.0 mm thick and the outer diameter of the target only about 30 mm. The thickness of the impactor determines how long the shock in the target can be maintained, before the release wave reflected from the liner surface, returns. Maintaining the velocity distribution for a longer time in the target permits more interface displacement, and more easily diagnosed experiments. More powerful machines were needed to drive thicker

liners, so that more satisfactory tests of the "friction" model could be designed.

The ATLAS pulsed power system has been operating at LANL since September 2001. Certification shots drove 27 MA of electrical current through an inductive load. Current rise time was 5-5.5 μs. Since then, experiments with imploding liners have been successfully conducted at current between 9-22 MA. With dynamic loads in a slightly higher inductance load region, the rise time of the bank is 6.0-6.5 μs. ATLAS provides enough energy to drive the experiments that we need to conduct thick-liner, friction studies.

We have chosen an impactor thickness of 10. mm as the design goal for these experiments. From simple incompressibility arguments, we can write down an algebraic expression that relates the final liner thickness, $\Delta_f = R_o|_f - R_i|_f$, to the initial liner thickness, $\Delta_i = R_o|_i - R_i|_i$, and the aspect ratio of the implosion. It is convenient to write this equation in terms of (a) the outer line radius, R_L, (b) the outer target radius, R_T (since $R_i|_f = R_T$!), and the final, impact liner thickness, Δ,

$$\Delta_i = R_L \{1 - (1 - \Delta(2R_T + \Delta)/R_L^2)^{1/2}\} \qquad (2)$$

Equation (2) indicates that there are a very large number of dimensions that satisfy this criterion, even if we fix the final thickness and the target radius. (An infinite number of solutions, actually!) As a concrete example, in order to have a liner that is 10 mm thick at the target surface (R = 25. mm), it should be fabricated to be 6.411 mm thick.

The final constraint on the design is that the liner should reach an impact velocity of 1.4-1.5 km/s when accelerated by the pulse-shape provided by the ATLAS pulsed-power system. A typical current pulse from ATLAS is shown in Figure 2. The current magnitude can be varied fairly easily, by varying the charging voltages on the system.

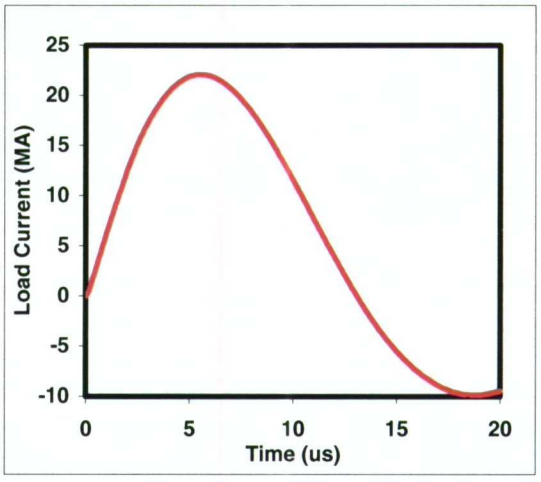

Figure 1. Typical load current waveform from ATLAS circuit model for 156 kV bank voltage.

Changing the gross time-scales of this pulse would require a major and uncertain re-design of the entire power-flow/load chamber design. For design purposes, this fixed time profile greatly reduces the number of acceptable liner parameter combinations.

The target geometry for ATLAS experiments will have a diameter of 40-54 mm, with a hollow opening in the center. The hollow core facilitates the placement of diagnostics to measure shock break-out, and to ameliorate axial jet formation. A typical target configuration is shown in Figure 1. The outer diameter of the initial aluminum liner design was 100 mm, but is being reduced to 88 mm for future shots. At 100 mm OD, the initial thickness will be between 5.73-6.87 mm thick, depending on the target diameter. In all cases, the liner

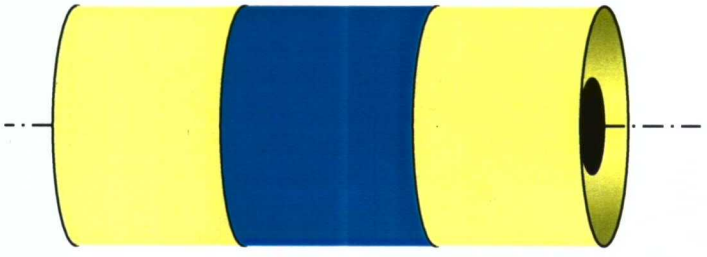

Figure 2. Typical target geometry, where the symmetric yellow materials have the slower sound speed, and the blue has a higher sound speed.

thickness at impact time will be ~10 mm.

The primary diagnostic for transverse shear during the plastic flow will be thin, soft, high- density wires embedded in the more radiographically transparent material (ie. Al). With present LANL x-ray sources, the Tantalum is too opaque to yield any radiography data. The Aluminum can be accurately imaged, however. With high-Z material such as lead (Pb) for the wires, the wire/Aluminum contrast will allow imaging of the wire motion. If, as expected, the soft wire deforms and flows with the Aluminum material, then the motion of the wires will provide direct evidence of the plastic flow of Aluminum under the forces induced by the interface friction. Comparison of the measured wire motion with 2-D hydrodynamic calculations will help confirm the validity of the friction model.

IV. Numerical Modeling Tools used to Design the Experiments.

Equation (2) was used to guide our parametric study of potential liner designs for the friction experiments. The basic assumption that underlies Eq. (2) is that the material in the liner remains incompressible, $\rho \cong \rho_o$. This is a reasonable assumption for planar, solid plates. In our converging geometry, however, the inner surface of the liner usually has a higher density that does the outside surface. The liner also experiences significant Ohmic heating from the currents that carry the magnetic fields, which implode the liner. This heating also changes the conductivity of the material, since for metals $\sigma \sim 1/T$, where σ denotes the conductivity and T the material temperature, in any absolute scale. This dynamic process is furthermore highly inhomogeneous, since the current begins by being localized on the outer liner surface, and then diffuses inward. Eq. (2) also neglects any effects associated with the interaction of the liner with the electrodes, or glide planes. To provide for more accurate designs that take into account the dynamic nature of a magnetically-driven liner implosion, we have utilized a suite of numerical tools.

A one-dimensional Lagrangian Resistive Magnetohydrodynamic code (RMHD) was used for the initial parameter studies, using Eq. (2) as a guide for promising dimensions. These calculations were fast enough to permit a broad survey of configurations, while retaining a full hydrodynamics treatment, including Steinberg-Guinan2 strength treatment, and a self-consistent magnetic field/current evolution throughout the current pulse. The key to accurate calculation of the magnetic field dynamics is an accurate model for the conductivity of the materials as a function of density, pressure, temperature, and ionization state, if appropriate. We have found the tables formulated by Desjarlais3 to yield results that are most consistent with data. Equation-of- State data was taken from the SESAME tables. The code also employs a circuit model for the ATLAS pulsed-power system. This feature permitted us to include the self-consistent behavior of the capacitor bank for different liner speeds and dimensions and bank charging voltages.

Liner deformation, instability, and interaction with the electrodes are all phenomena which are relevant to accurate liner design, but which are beyond the scope of 1-D calculations. To address such issues, we employed a two-dimensional RMHD Eulerian code [7]. The physics models in this package have been described elsewhere. We have employed a newer version of this package, which uses Automatic Mesh Refinement (AMR) to provide the highest resolution at locations involving the greatest gradients. This technique is potentially faster and less cumbersome than simpler algorithms that require very fine resolution everywhere to achieve the same quality of numerical solution.

Finally, the object of the experiments is to test our friction model, not to test liner performance. The Eulerian code described above treats multi-material interfaces through a mixed cell treatment. This treatment models the interface of two materials by a suitable averaging of the

individual constituents of the interface. For many applications, this treatment has proved to give physically reasonable results. For a quantitative test of the transverse shear stresses at the interface between two dissimilar materials, however, we feel that a different numerical technique is required. We have chosen to use a two-dimensional Lagrangian, hydrodynamics code, for which the interface forces between two materials (or regions in this case) can be explicitly controlled. The use of these controls implicitly presupposes certain transverse forces. We will use this code to check against the data. By varying the interfacial forces, we will obtain a quantitative value for this force, which will be compared against the friction model. The calculations were "driven" by a circuit model of the ATLAS pulsed-power system. A typical current waveform from this circuit model is Figure 2.

The calculation closely approximates the current waveform measured during ATLAS tests. Note that current reversal occurs at about 13 μs. This is significant because some of these very thick liner designs do not impact the target until 18-20 μs. Behavior of these liners during current reversal should prove interesting.

A. 1-D RMHD Numerical Study

A series of 1-D RMHD calculations were conducted to obtain inner surface velocity, time of impact, and internal distribution of temperature, pressure, and density, subject to the constraint that the liner is 10. mm thick at the time of impact. Eq. (2) was used to obtain the initial liner thickness for different initial outer liner radii. A circuit solution that accounted for liner motion (and hence a time varying load inductance) was used in these calculations. The circuit parameters used to model ATLAS were 816 nF capacitance, 21.5 nH of inductance and a total series resistance of 0.05 Ω. The basic experimental parameters, liner thickness, liner radius, target radius, and peak current were derived from the 1-D calculations, with the ATLAS bank voltage being the independent variable, used to vary load current. All design calculations were conducted subject to the constraint that the impact velocity of the liner on the target should be 1.4-1.5 km/s and the liner should be 10 mm thick.

The evolution of the liner and target surfaces as calculated from one promising design is shown in Figure 3. This

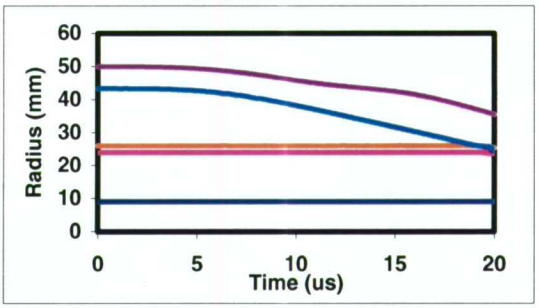

Figure 3. Time history of liner surfaces, starting at outer radius of 50. mm, hitting a 2.0 mm shock pad, and target that extends 10-24 mm.

configuration has an outer liner radius of 50.0 mm and a target outer radius of 26. mm. The corresponding velocity history of the liner's inner surface is shown in Figure 4. It should be noted that the liner reaches 95% of its peak velocity by time 13.0 μs

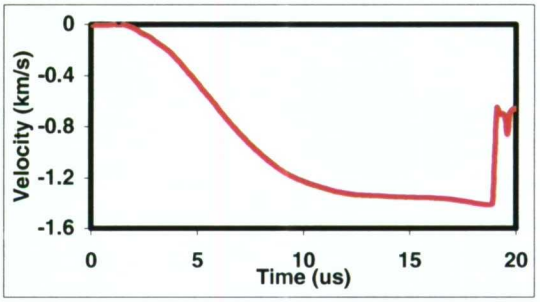

Figure 4. Time history of velocity of the inner liner surface, shown in Fig. 3.

(current reversal). It has traveled only 9.09 mm by this time. Since the initial distance between liner and target was 17.3 mm, additional time was required to reach the target, during which the liner essentially coasted ballistically. The choice of 50.0 mm for an initial liner radius is motivated by our intention to maximize the liner/glide plane interaction, to assess any effects related to current reversal, and to validate our

numerical design tools. This last will be discussed more in Section IV.B.

The fact that these thick liners almost reach the limiting velocity much earlier in the waveform (c.f. Figs. 1 and 4), suggests that a liner could satisfy the target impact velocity with a reduced initial liner radius. Such an experiment could be designed to impact the target before current reversal. Detailed calculations confirm this. For instance, a liner that is initially 8.0 mm thick, with a 44.0 mm outer radius is predicted to reach a 27.0 mm radius target at 12.4 μs. At that time, the 1-D calculations yield an inner surface velocity of 1.48 km/s.

Parametric numerical studies have been conducted to better understand the range of acceptable liner designs, subject to the above- discussed constraints, driven by an ATLAS waveform. An example of the type of information that this yields is shown in Figure 5. These studies examined the

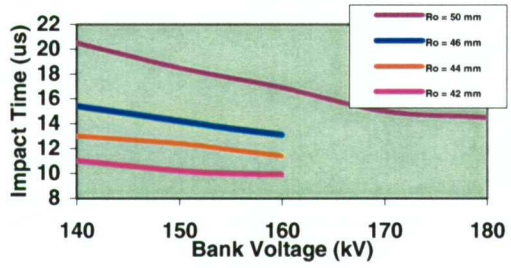

Figure 5. Variation in impact time for different initial liner outer radii, subject to Eq. (2) and a final thickness of 10 mm.

variation of bank charging voltage, of initial liner radius, and of target radius. This last has practical significance, because extant LANL radiographic sources do not provide adequate contrast when the chordal thickness of the liner/target assembly is too thick. Smaller targets give better X-ray transmission with the photon spectrum of existing sources.

During early operations at ATLAS, it is expected that peak currents will be limited to about 22 MA, which corresponds to about 155 kV for these thick liner loads. It is not known certainly at this time what the lower voltage limit for reliable triggering will be, so 145 kV is a conservative lower bound.

B. 2-D MHD Numerical Study

The significant interaction between these thick liners and the electrode walls was not treated in the 1-D calculations. To better estimate the long-time (~15-20 μs) interaction effect, two-dimensional MHD calculations were performed to investigate liner/wall phenomenon.

Steinberg-Guinan strength models [ref] are employed for all materials. Other, more sophisticated strength models exist, but the liner should experience only modest strains and strain rates. From the 1-D calculations, we expect that the liner will be strained about 45% by the time it has imploded to the radius of the target. Similarly, the strain rate is predicted to be less than 10^5 s^{-1}. Steinberg-Guinan is probably adequate for these conditions.

Different ways of "mounting" the thick liner on the electrodes have been modeled. Figure 6 shows three of these. In Fig.6(a) the liner is a simple cylindrical tube of aluminum liner, which sits on top of the electrode outer surface. A potential issue with such a design is that the liner must shear through 6-8 mm of material before it is fully detached and imploding. This indeed

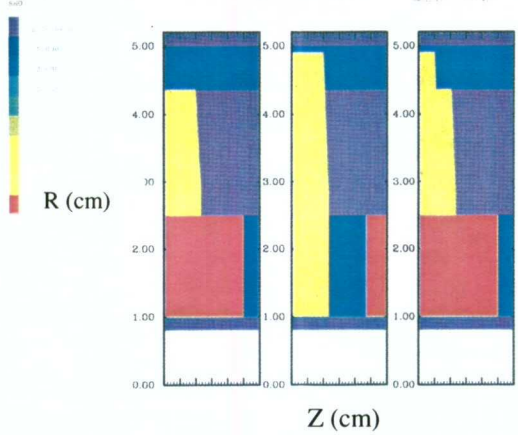

Figure 6. Different configurations used to mount a thick liner on the electrodes, (a) Uniform aluminum tube, $4.36 \leq r \leq 5.00$ cm, (b) Thin aluminum shell, 0.10 cm thick, sitting on electrode with radius, 4.90 cm, rest of liner 'hanging' between electrodes, (c) Compromise between designs (a) and (b); Z-axis runs fro, 0.0 to 3.0 cm.

proved to be a major problem when copper (Cu) electrodes were used. The deformation of the electrodes (!) was judged to be unacceptable. We decided to fabricate the electrodes from a specially heat-hardened Stainless Steel alloy (416), which has a basic yield limit of over 100 GPa. Use of this electrode material has reduced the electrode deformation to a manageable level.

The design shown in Fig. 6(b) avoids this massive shearing issue by placing only one millimeter of liner on top of the liner, with the rest "hanging" down into the glide plane region. This particular configuration has already been tested on ATLAS.

That experiment uncovered an unexpected issue in the operation of ATLAS. Because of the high energies involved in a high voltage ATLAS experiment (10-15 MJ), extensive inertial damping and blast protection was provided in the load region. The mechanical stresses apparently coupled into the load mounting, however. As Figure 7 shows, the mass loading on top of the load region resulted in significant separation between the "hanging" section of the liner and the electrode wall (~3 mm). The portion of 1.0 mm thick "liner" ran well ahead of the bulk and resulted in early time current breaching into the interior of the

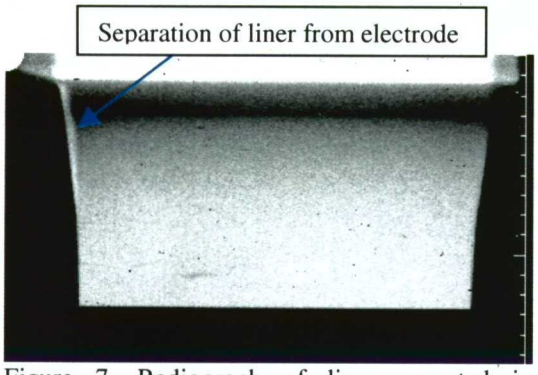

Figure 7. Radiograph of liner mounted in configuration Fig. 6(b), showing electrode/liner separation.

liner. (The current joint for this mounting involved a "shrink fit" of the liner onto the electrode, so pushing the electrodes together was not an option!) This clearly undesirable feature has made us cautious about fielding any more thick liners with this type of electrode mounting.

In Fig. 6(c), a compromise design was found. This design protected the liner from mechanical wall separation, but also requires almost as much shearing as the design in Fig. 6(a). Fig 8 shows the liner deformation of all three designs, shortly before impact with the target. There is remarkably little difference in the inner surface shape of the

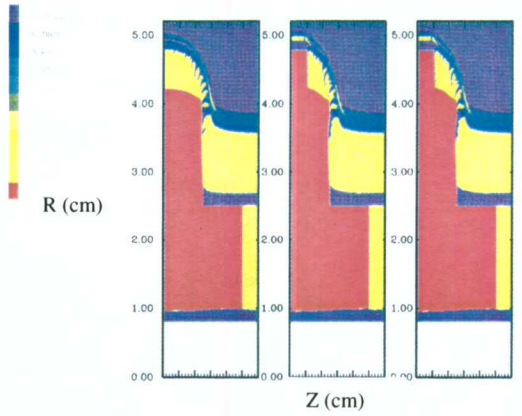

Figure 8. Evolution of the three liner configurations shown in Fig. 6, shortly before impact with the target (~19. μs after current initiation); Z-axis on all figures runs from 0.0 to 3.0 cm.

aluminum liner, despite a significant deformation of the electrodes from their original shape.

A typical velocity distribution in the target (Same as Figs 6(a), 8(a)) is shown in Figure 9. The velocity field in the denser

Figure 9. Velocity field in the target, approximately 3.0 μs after liner impact with its surface, from calculation shown in Fig. 8(a).

material (Ta) is obscured by the bow shock from the pressure wave in the aluminum.

Finally, we show the interfaces alone for the calculation represented by Figure 9. Note that the harder Tantalum has extruded into the soft aluminum. It is essential that

Figure 10. Material interfaces are shown alone, to illustrate the radiographic obscurance induced by the extrusion of higher density Ta into the aluminum, from calculation shown in Fig. 9.

the actual interface be visible on radiographs to obtain good data on the interface shear flow. If the deformation of the soft lead (Pb) pins can not be discerned, the value of the data is severely compromised. The extrusion of the Ta shown in Fig 10 would hide the very region that we need to measure. It seems highly likely that we will need to modify the *initial* shape of the Al-Ta interface, so that the *final* shape is close to straight.

VI. Summary

A new model for the transverse, sliding forces between two solid interfaces has been proposed. The critical speed differential is accessible with liner/target experiments being designed for the ATLAS pulsed power system. Liners with unprecedented thickness are required to sustain shocks in multi-material targets. One-dimensional MHD calculations indicate that there will be a significant spectrum of design parameters that should yield successful liner performance. The design constraints are (1) that the liner should be 10 mm thick at the time of liner impact with the target, (2) that the inner surface velocity should be 1.4-15 km/s, and (3) that the inner surface should be flat. Two-dimensional MHD calculations performed to evaluate the large interaction between the liner and the electrode walls, confirm the "flatness" of the liner at impact time. ATLAS experiments are scheduled for the end of FY02 at LANL.

VI. References

[1] J. E. Hammerberg, B.L. Holian, J. Rider, A.P. Bishop, S.J. Zhin, "Nonlinear dynamics and the problem of slip at material interfaces," Physica D233, 336-340, 1998.

[2] R.E. Reinovsky, "Pulsed Power Experiments in Hydrodynamics and Material Properties," Proc. 12th IEEE Int. Pulsed Power Conf (ed., C Stallings and H. Kirbie), 38-43, 1999.

[3] J.E. Hammerberg and B.L. Holian, "Simulation Methods for Interfacial Friction in Solids," in Surface Modification and Processing Physical and Chemical Tribological Methodologies (ed,. G.E. Tollen and H. Liang), New York, Marcel Dekker.

[4] J.E. Hammerberg, T.C. Gormann, B.L. Holian, "Modeling High Speed Friction at Ductile Metal Interfaces," Proc. Int. Workshop on New Models and Hydrocodes for Shock Wave Processes in Condensed Matter (ed. I.V. Klimenko) (to be published).

[5] J. Röder, T. Gormann, J.E. Hammerberg, B.L. Holian, "Sliding between two incommensurate workpieces," (to be published)

[6] D. Steinburg, Lawrence Livermore National Laboratory Publication No. UCRL-MA-106439, February 13, 1996.

[7] R.L. Bowers, A.E. Greene, D.L. Peterson, N.F. Roderick, R.R. Bartsch, J.C. Cochrane, and H. Kruse, IEEE Trans. Plasma Science **2**, 510 (1996).